Adverse Rotorcraft-Pilot Coupling: Recent Research Activities in Europe

Oliver Dieterich
Eurocopter Deutschland GmbH
oliver.dieterich@eurocopter.com

Joachim Götz
DLR
joachim.goetz@dlr.de

Binh Dang Vu
ONERA
binh.dangvu@onera.fr

Henk Haverdings
NLR
haverdi@nlr.nl

Pierangelo Masarati
Politecnico di Milano
pierangelo.masarati@polimi.it

Marilena Pavel
Technical University of Delft
m.d.pavel@tudelft.nl

Michael Jump
University of Liverpool
mjump1@liverpool.ac.uk

Massimo Gennaretti
Università Roma Tre
m.gennaretti@uniroma3.it

Key words: APC, RPC, PIO, pilot-in-the-loop, rotorcraft-pilot coupling

Abstract: Unintended and unexpected oscillations or divergences of the pilot-rotorcraft system have become a critical issue for augmented helicopters with modern flight control systems. The rapid advances in the field of high response actuation and highly augmented flight control systems have increased the sensitivity to aspects that lead to complex oscillations related to unfavourable Aircraft-Pilot Coupling (APC) and Rotorcraft-Pilot Coupling (RPC) events. The understanding, prediction and prevention of adverse RPCs are demanding tasks and require the analysis and simulation of the complete feedback loop: pilot – control system – rotorcraft. Based on numerous flight events in the past, several types of RPCs have been observed differing in their frequency content as well as in the underlying physics and human behaviour.

In Europe, research activities were launched in 2005 under the umbrella of the GARTEUR organisation in order to improve the physical understanding of RPCs and to define criteria for quantifying the helicopters susceptibility to RPC. This paper is intended to give an overview of the various numerical and experimental activities of the research group. Selected results are highlighted and discussed demonstrating the approach used to investigate different RPC phenomena in a systematic manner.

Nomenclature

APC	Aircraft-pilot coupling
MIMO	Multiple input – multiple output
OLOP	Open loop onset point (criterion)
PAO	Pilot assisted oscillations
PIO	Pilot induced oscillations
PIOR	PIO rating
RCAH	Rate command – attitude hold
RPC	Rotorcraft-pilot coupling
SISO	Single input – single output

1. INTRODUCTION

During the last decade there has been an increase in research with regard to the causes and remedies for oscillations or divergence phenomena due to adverse vehicle-pilot couplings. These events may be better known in the aircraft and rotorcraft community as Pilot Induced Oscillation (PIO) and Pilot Assisted Oscillation (PAO), whereas divergence-type events are less known in practice. The urgent need for an efficient engineering understanding and for

solutions for the APC / RPC problem stems from incidents and catastrophic accidents in the past, see [1, 2, 3]. The understanding, prediction and prevention of adverse RPCs are demanding tasks and require the analysis and simulation of the complete feedback loop: pilot - control system - rotorcraft. Based on numerous flight experiences in the past, different types of RPCs have been observed, which are simplified in this paper to 'rigid body' RPCs – the realm of flight dynamics – and 'aeroelastic' RPCs – the realm of aeroservoelasticity. It is assumed that a certain overlap between these two RPC categories exists. In a first approach, these two types can be distinguished by different frequency ranges.

The lower frequency range in the vicinity of and below 1Hz is emphasized by adverse coupling phenomena dominated by helicopter low frequency dynamics i.e. the field of flight mechanics, by the flight control system and by an 'active' pilot concentrating on performing his mission task by actively manipulating the helicopter controls. The higher frequency bandwidth at 2Hz up to 8Hz is characterised by higher helicopter frequency dynamics i.e. the inclusion of elastic airframe and main rotor blade modes, by a 'passive' pilot subjected to vibrations which are too high in frequency to adequately be reacted by human beings and by the cockpit controls layout affecting the pilots inertial response on the helicopter control elements. For the overlap between 1Hz and 2Hz the classifications of rotorcraft-pilot coupling mentioned above lead to a merge of phenomena where a mix of models and procedures will be more adequate. Initial ideas for closing this gap were developed and discussed within the group. Nevertheless, in the paper, numerical and experimental research activities will be presented using this clear distinction for simplicity. Table 1 summarises the distinctions made.

	Rigid Body RPC	**Aeroelastic RPC**
Frequency Range	Below 1Hz	Between 2Hz and 8Hz
Pilot Behaviour	'Active' pilot concentrating on a task	'Passive' pilot subjected to vibrations
Helicopter Dynamics	Flight mechanics	Structural dynamics
Critical Components	Flight control system	Airframe modes

Table 1: Characterisation of 'Rigid Body' and 'Aeroelastic' RPC

The numerical studies were performed using a BO105 model which served as a numerical test bed for all of the partners. Although well known that the full scale BO105 is not prone to RPC issues, the BO105 theoretical model was applied with additional numerical degradation of its characteristics in such a way as to provoke different types of unfavourable RPC. In order to complement this theoretical work experimentally, a 6dof motion base flight simulator at the University of Liverpool was used, see Fig. 1.

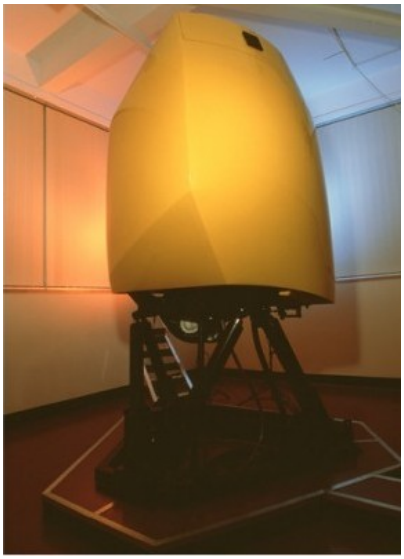

Figure 1: The "Bibby" flight test simulator – University of Liverpool

The application of the flight test simulator for this purpose is favourable as it uses exactly the same numerical helicopter models for prediction and experiment thus allowing the validation of pilot models and PIO criteria to be the main focus of the research. Flight test simulator campaigns were performed for the analysis of the pilot ratings in RPC prone operation environment and for the determination of the pilot transfer behaviour aiming on coupling problems of the 'passive' pilot. A simulation test approach was developed including the structural dynamics properties of the airframe as well as for simulations of 'aeroelastic' RPC.

Participating partners of the research group are:

- ECD (co-ordinator) and DLR from Germany
- ONERA from France
- NLR and the Technical University of Delft (TUD) from the Netherlands
- Politecnico di Milano (POLIMI) and Università Roma Tre (UROMA3) from Italy
- University of Liverpool (UoL) from the UK.

The partners shared the main activities in the group as follows:

- Set-up of BO105 database: DLR and ECD
- 'Rigid body' research activities: ONERA, TUD and UoL
- 'Aeroelastic' research activities: ECD, POLIMI and UROMA3

The overall objectives of the research activities relate to the establishment of guidelines for the development of means to prevent or suppress critical RPC incidents in future thus contributing to increased helicopter operational safety. In detail these objectives are

- Improvement of the physical understanding of RPC
- Definition of criteria to quantify the susceptibility to RPC
- Development of prediction methods for RPCs
- Validation of prediction methods and criteria
- Development of preliminary guidelines/recommendations/methods for RPC prevention/suppression

Focus was given on the one hand to RPC phenomena in the frequency range up to approximately 1Hz and on the other hand to coupling phenomena roughly between 2Hz and 8Hz.

This paper is intended as an overview paper presenting the different activities and their dependencies. More detailed information on 'rigid body' RPC can be found in [4] while [5] is dedicated to an in-depth treatment of 'aeroelastic' RPC. Reference [6] presents the experimental activities related to 'rigid body' and 'aeroelastic' RPC with the flight test simulator as a core device for the test activities. The different activities were bracketed on the one hand by the numerical helicopter database and on the other hand by the flight test simulator as the main experimental tool for RPC research.

2. THE 'NUMERICAL' TEST BED

For the application of different methodologies and tools, a common database of the BO105 helicopter – see Fig. 2 for the helicopter – was created allowing the partners to set up the helicopter models according to the code capabilities. The BO105 database consists of five volumes comprising helicopter configuration data, flight test data, identified state space models, main rotor aeroelastic data and elastic airframe data.

Figure 2: DLR BO105 research helicopter used for flight tests and system identification

The BO105 is a small multipurpose helicopter built by formerly MBB (now Eurocopter) and is powered by two Allison 250 C20 engines. It is a relatively small helicopter with an empty weight of about 1200kg and a maximum gross weight of 2300kg. Typical uses of the highly manoeuvrable BO105 helicopter are transport, offshore, police, and military missions. The BO105 has a four-bladed hingeless main rotor of 4.9m radius and a two-bladed teetering tail rotor. The composite blades of the main rotor have a very high equivalent hinge offset giving the BO105 an extremely high bandwidth and excellent manoeuvrability in the roll and pitch axes. The semi-rigid teetering tail rotor is on the left side of the helicopter operating as a pusher. The pilot control inputs are augmented by two parallel hydraulic servo systems. There is no specific mixing unit, so that control inputs are only mixed at the swash plate.

The BO105 helicopter configuration database consists of configuration data for the global helicopter, for the fuselage including horizontal and vertical stabiliser, for the main and tail rotor systems and for the control system. Aerodynamic data in tables are also presented in coefficient form for the fuselage, the horizontal and vertical stabiliser and main and tail rotors. Thus, sufficient information is given by this database for a 'flight mechanics' model of the BO105 featuring a rigid airframe, a rigid main rotor model with equivalent hinges and a teetering rigid tail rotor to be established. This model is representative for baseline applications within the scope of 'rigid body' RPC.

The flight tests that resulted in the BO105 flight test database were conducted in 1987 for system identification and simulation validation purposes. For the generation of the database the helicopter was equipped with a pair of strain gauges on all the four blades at the location of the equivalent hinge offset to measure the blade tip deflection. This database is built up for system identification purposes and is restricted to the flight test condition of 80kts. The selected data consist of:

- positive and negative doublet inputs for each of the four controls
- positive and negative modified 3-2-1-1 inputs for each of the four controls
- pilot generated frequency sweeps for each of the four controls

The flight test database is intended to provide the partners with experimental data for correlation activities of their numerical helicopter models.

The BO105 state space model database describes the following two state space models identified in flight:

- 12 degrees of freedom model in hover
- 12 degrees of freedom model for level flight (65kts or 33m/s)

of the DLR research helicopter BO105 S123. The differential equations of motion, describing perturbed motion around the working point of the general trim condition, can be written as:

$$\dot{x} = Ax + Bu \tag{1}$$

where x is the state vector:

$$x^T = (u\ v\ w\ p\ q\ r\ \varphi\ \theta\ \psi\ \dot{p}\ \dot{q}\ \dot{r}) \tag{2}$$

and u the control vector:

$$u^T = (\delta_x\ \delta_y\ \delta_0\ \delta_P) \tag{3}$$

The state vector x is composed of the following components:

- u, v and w are the translational velocities along the three orthogonal directions of the body fixed axes system.
- p, q and r are the angular velocities around the x-, y- and z-axis.
- φ, θ, and ψ are the Euler angles, defining the orientation of the body axes relative to the earth.

The control vector u with the pilot controls has four components and is given in %:

- δ_x is the longitudinal pilot control: -100% pushed +100% pulled
- δ_y is the lateral pilot control: -100% left +100% right
- δ_0 is the collective pilot control: 0% pushed down +100% pulled up
- δ_p is the pedal pilot control: -100% pushed left +100% pushed right

As shown in equation (1) and (2) the differential equations for roll, pitch and yaw (yaw not used) are extended to equations of second order. Starting from the standard differential equation for roll and pitch:

$$\dot{p} = L_p p + L_{\delta_y} \delta_y \tag{4}$$

$$\dot{q} = M_q q + M_{\delta_x} \delta_x \tag{5}$$

the following differential equation of second order with the roll and pitch time constants (τ_p and τ_q are generated:

$$\tau_p \ddot{p} = -\dot{p} + L_p p + L_{\delta_y} \delta_y \tag{6}$$

$$\tau_q \ddot{q} = -\dot{q} + M_q q + M_{\delta_{xy}} \delta_x \qquad (7)$$

and added to the standard fixed body model. With this extended fixed body model (eq. (1) and (2)) the short time response from the rotor body coupling is approximated. The long time response of the equations (4) and (5) is equal to the response of the equations (6) and (7) since the right hand side of the equations (6) and (7) is zero.

In the main rotor aeroelastic database, information is presented for setting up a BO105 main rotor model as single load path model based on beam properties. The database contains cross section characteristics along the rotor radius such as

- flap, lag and torsion stiffness properties including structural twist angle
- section mass, section moment of inertia and section polar inertia properties including inertia twist angle
- axes offset definitions for shear centre, tension centre and centre of gravity offsets
- aerodynamic chord and twist distributions.

Furthermore point mass definitions for lumped masses are included as well. The modeling of a detailed swashplate mechanism (including the pitch horn) is assumed not to be required for RPC studies due to high stiffness of the rotor hub thus leading to neglectable pitch-flap and pitch-lag coupling terms. Furthermore, the blade flap pendulum absorbers are not included in the description for simplicity reasons. Figure 3 shows a fan diagram based on the aeroelastic database comparing aeroelastic modes in baseline atmosphere and in vacuum conditions – i.e. without air loads.

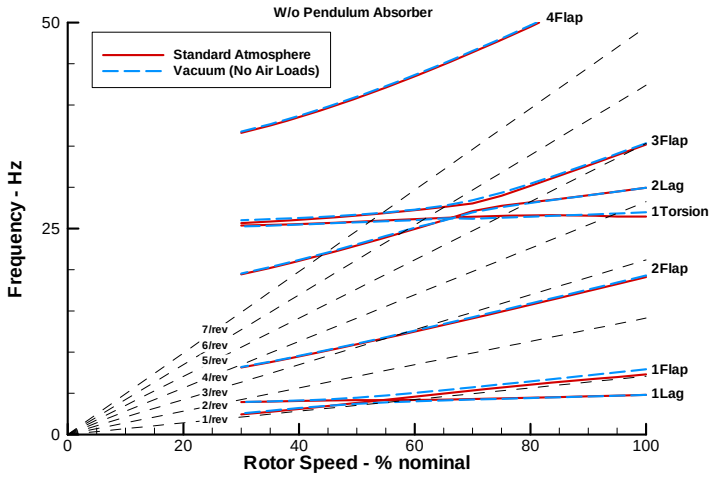

Figure 3: Fan diagram of BO105 aeroelastic rotor model

The database for the elastic airframe is derived from a NASTRAN Finite Element analysis of the BO105 model. Related experimental and theoretical results for the BO105 airframe are described in [7]. Compared to today's finite element modelling practice of helicopters, the model of the BO105 airframe is very coarse, see Fig. 4. For the activities envisaged with respect to RPC, focus was given to the fundamental bending modes of the fuselage due to the location of the corresponding natural frequencies below 10Hz, see also Table 2. For these low frequency modes, the model shows adequate performance. Please note that the theoretical results (and also the applied finite element model) presented in this document slightly differ from the results of [7] for two reasons: First, the fuselage of the BO105 ran through different modifications during the production phase. Second, a crew of two persons is considered in the model used for extraction of modal data for this document.

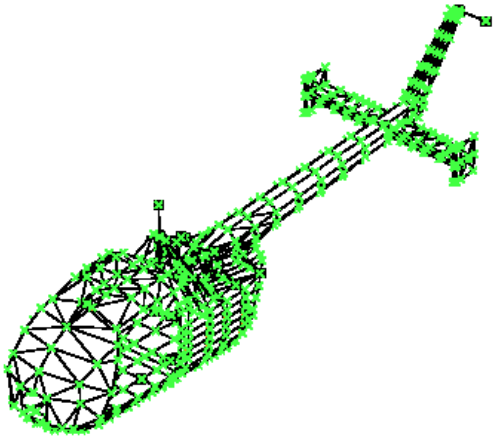

Figure 4: BO105 Finite Element Airframe Model

The description of the elastic behaviour of the airframe is based on modal data consisting for each mode of values for

- modal mass and frequency
- mode shape vectors at main and tail rotor hubs
- mode shape vectors at pilot and co-pilot seat locations

Mode	Frequency – Hz	Mode Shape
1	5.80	Fundamental fuselage pitching mode
2	7.68	Fundamental fuselage lateral mode
3	11.42	Higher airframe mode
4	12.57	Higher airframe mode

Table 2: Frequencies for the first four airframe modes – NASTRAN results

The damping level of the various modes can not be retrieved by the finite element analysis as damping is not appropriately included. Although damping will vary for the different modes, the assumption of 1% or 2% critical damping is an adequate estimation within these activities.

3. 'RIGID BODY' RPC

In the framework of this paper 'rigid body' RPC is understood to cover coupling phenomena between the rotorcraft and the pilot at frequencies of approximately 1 Hz and below. The wording 'rigid body' refers to the helicopter as a rigid structure which is – depending on the investigated theoretical model – not totally true as rotor flapping might be considered as well by additional degrees of freedom. In fact, the peculiarities of main rotor aerodynamics and dynamics lead to significant differences in the behaviour of rotorcraft compared to fixed wing aircraft. Due to asymmetries in the aerodynamic environment of the main rotor blades in forward flight no symmetries in the equations of motion exist for the helicopter and cross-coupling terms between all axes appear. Furthermore, due to flexibilities of the rotor system e.g. introduced by articulation of the rotor blades or in the case of the BO105 by flexible blades, the main rotor tip path plane is generally oriented differently in space compared to the airframe. Thus the underlying dynamic behaviour of the rotor tip path plane is different from

the airframe introducing some lagging terms in the equations of motion. These differences mean that existing knowledge of RPC in the fixed wing world cannot be transferred directly to the rotorcraft world without verification and/or adjustment. Therefore the main research focus with respect to 'rigid body' RPC was to review the existing PIO criteria for fixed wing aircraft and to assess whether these criteria could be applied to rotorcraft with or without modification. In this context, it should be mentioned that most of the PIO criteria of interest for this research are known as category I PIO criteria in the fixed wing world i.e. they deal with linear system behaviour and characteristics. One category II PIO criterion was analysed as well investigating saturation effects with respect to main rotor control. Category III PIO criteria related to flight control system state transitions etc. were beyond the scope of the research activities.

The methodology of checking PIO criteria for rotorcraft usage within these research activities was based up on a multiple step approach. First, the numerical helicopter models were modified by introducing an artificial flight control system in order to present a large bandwidth of flight dynamic characteristics affecting RPC. Second, the modified helicopter models were imported into the simulator and flight tested by professional test pilots. The pilots rated the different helicopter models based on a PIO rating scale and the ratings were cross-checked with the predictions obtained by the different PIO criteria. In case of insufficient correlation levels, the question how to modify the criteria in order to better fit the experimental results was addressed.

The 'rigid body' RPC activities are highlighted in this chapter by two issues, the modification of the BO105 helicopter model and the application of various PIO criteria to the modified rotorcraft models. The input for the set-up of 'rigid body' helicopter models is mainly given by the configuration database while the flight test database can be used for validation of the models. Alternatively, the state space models identified by flight tests can be applied directly but only for selected flight conditions. In a first step, the partners involved in 'rigid body' RPC research compared their models with respect to eigenvalues and the results of three different PIO criteria. Observed differences are mainly due to varying order of the models e.g. TUD applied an eighth order model, DLR used a tenth order model and ONERA a twelfth order model. Next, a simple flight control system of RCAH type (rate command – attitude hold) was introduced into the numerical model of the BO105. The numerical flight control system allows the dynamic behaviour of the BO105 model to be modified in a straight forward manner. 12 different configurations of the flight control system were set up by ONERA, see Table 3 assigning Cx=C1 to forward flight (65 kts) and Cx=C2 to hover conditions.

Label	Flight Control System	FCS Dynamics	Time Delay
CxB-B	No -> **B**aseline model	N/A	200 ms -> "**B**ad"
CxB-M	No -> **B**aseline model	N/A	100 ms -> "**M**edium"
CxB-G	No -> **B**aseline model	N/A	0 ms -> "**G**ood"
CxA-L-B/M/G	Yes -> **A**ugmented model	**L**ow bandwidth	200/100/0 -> **B/M/G**
CxA-M-B/M/G	Yes -> **A**ugmented model	**M**edium bandwidth	200/100/0 -> **B/M/G**
CxA-H-B/M/G	Yes -> **A**ugmented model	**H**igh bandwidth	200/100/0 -> **B/M/G**

Table 3: Modified BO105 models for 'rigid body' RPC studies

Afterwards, different fixed wing PIO criteria were applied to the modified BO105 models. The related routines were previously developed and maintained in form of a PIO toolbox by action groups 12 [8] and 15 [9] under the flight mechanics umbrella of GARTEUR and were

made available for this activity to the helicopter group. The following PIO criteria have been tested with respect to the modified BO105 models:

- bandwidth-phase delay criterion
- average phase rate criterion
- Gibson frequency domain criterion
- OLOP criterion

For detailed descriptions of the PIO criteria see Ref. [10]. Figure 5 shows results for the average phase rate criterion concerning the pitch axis. As it can be seen from the labels (C1…) of the different entries the figure is related to the forward flight case. The lines separate bands of different ratings with the lower right area representing best behaviour and the upper left band representing most unfavourable behaviour. From fixed wing databases it is experienced that the PIO rating of a configuration is very likely less than 2.5 if the criterion parameters are located within the Level 1 area. As expected low dynamics (identifier L) and high time delays (identifier B) of the flight control system lead to a significant degradation of the coupled system with respect to the PIO criterion.

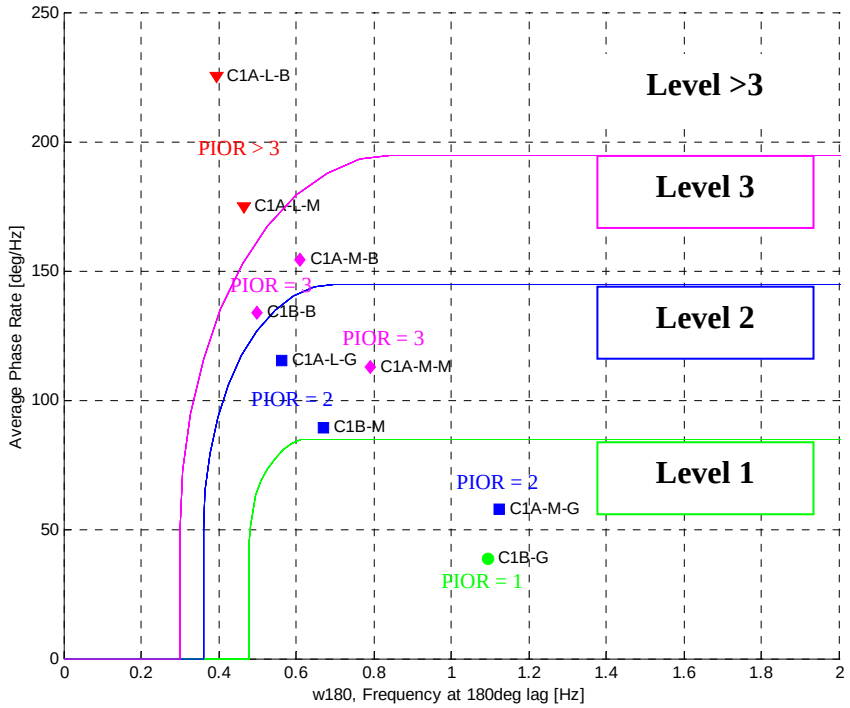

Figure 5: Average phase rate criterion for pitch axis in forward flight – ONERA

Similar trends are also obtained by application of the bandwidth/phase delay criterion to the roll axis in hover, shown in Fig. 6. Consistent to the above figure, low dynamics and high time delays of the flight control system are unfavourable with respect to RPC. It was the objective of the flight simulator tests to check whether the boundaries indicated in the figures for separating favourable and unfavourable characteristics regarding RPC are adequate for rotorcraft. Other criteria were studied as well with respect to their applicability to rotorcraft such as the boundary avoidance concept analysed by TUD in depth. For more details of the investigated criteria see [4].

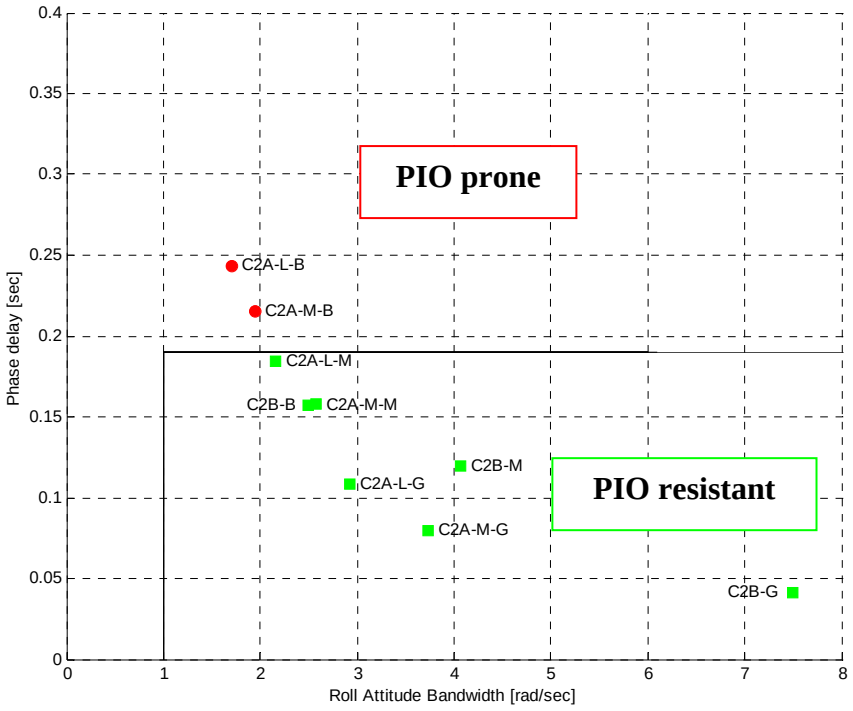

Figure 6: Bandwidth phase delay criterion for roll axis in hover conditions – ONERA

4. 'AEROELASTIC' RPC

Within the scope of this paper, 'aeroelastic' RPC is intended to cover coupling phenomena between the rotorcraft and the pilot at frequencies of approximately 2 Hz and higher. The wording 'aeroelastic' already reflects the impact of elastic structures of the rotorcraft on the dynamic characteristics of the coupled rotorcraft – pilot system. Typically, the main rotor and fuselage are the main structural components that have a significant impact on this kind of phenomena. Thus, an adequate modelling approach has to take into account fuselage flexibility and the elastic main rotor system in addition to the rigid body degrees of freedom. Regarding the pilot, the considered frequency range does no longer allow coordinated inputs from human beings. Instead the pilot reacts more or less in a passive manner being excited by the vibrations mainly experienced through the seat and interacting with the controls due to these vibrations. Pilot models for this kind of RPC phenomenon are totally different in nature from 'active' pilot models and, in a first approach, no longer mission task oriented. Therefore, this section is intended to give some highlights on the aeroelastic rotorcraft model embedded in an adequate closed loop system and on the set-up of appropriate pilot models. Nevertheless – depending on the specific RPC problem to be investigated – additional components with dynamic impact have to be considered as well in modelling such as

- actuator dynamics
- flight control system
- upper modes of drive train and engine control system
- upper modes of slung loads if present e.g. cable extension mode

Furthermore, it is expected that a 'grey' area exists with respect to the upper frequency boundary of 'rigid body' RPC and the lower frequency boundary of 'aeroelastic' RPC where 'rigid body' RPC and 'aeroelastic' RPC merge into a combined RPC phenomenon. In this

area, helicopter and pilot models have to combine the dynamic characteristics of both ‘rigid body’ and ‘aeroelastic’ RPC in order to appropriately treat the problem.

Generally – concerning ‘aeroelastic’ RPC – more detailed information is given in [5] which is dedicated to an in-depth presentation of the research work done in the context of ‘aeroelastic’ RPC.

4.1 Rotorcraft-Pilot Coupled System

Due to the impact of airframe structural modes on the occurrence of this kind of RPC, helicopter size will play a major role with respect to the classification of coupling phenomena. For light helicopters, a phenomenon called vertical bouncing is known to be of certain significance in the real world, describing the interaction of the collective control loop with vertical accelerations. Nevertheless the full scale BO105 is not known to show vertical bouncing. Furthermore – for rotorcraft of larger size – other RPC phenomena are more pronounced, see also [3]. The simplest mathematical model representing vertical bouncing is shown below in Fig. 7. The helicopter plant model consists of a single input – single output (SISO) system featuring collective control as input and pilot seat vertical acceleration as output. To complement this, the pilot model is also a SISO system showing vertical pilot accelerations as input and collective control as output. A slider gain block is introduced in addition in order to allow for increasing feedback gain and thus to set up root locus plots.

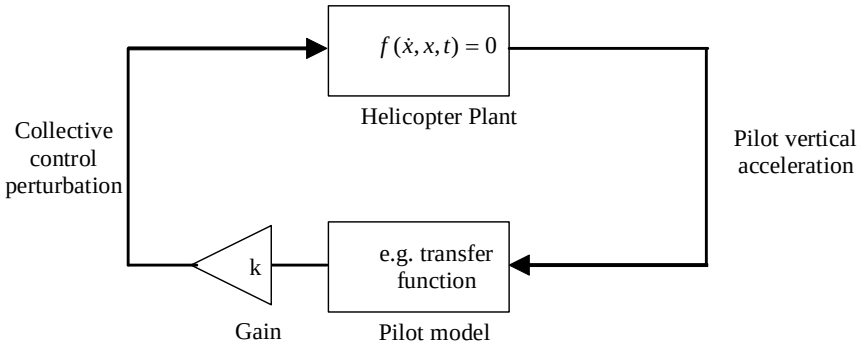

Figure 7: Closed loop system representing a simplified vertical bouncing system

The helicopter plant model is typically derived in state space form from comprehensive rotor codes by linearization of a trimmed BO105 numerical model as performed by ECD and UROMA3. POLIMI uses a slightly different approach based on a multibody model of the plant. In this case instability is assessed by identifying the response of the coupled system, integrated in time. Figure 8 shows a transfer function derived from a linearised plant model. The significant peak in the gain is related to the first elastic airframe mode which is a vertical bending mode.

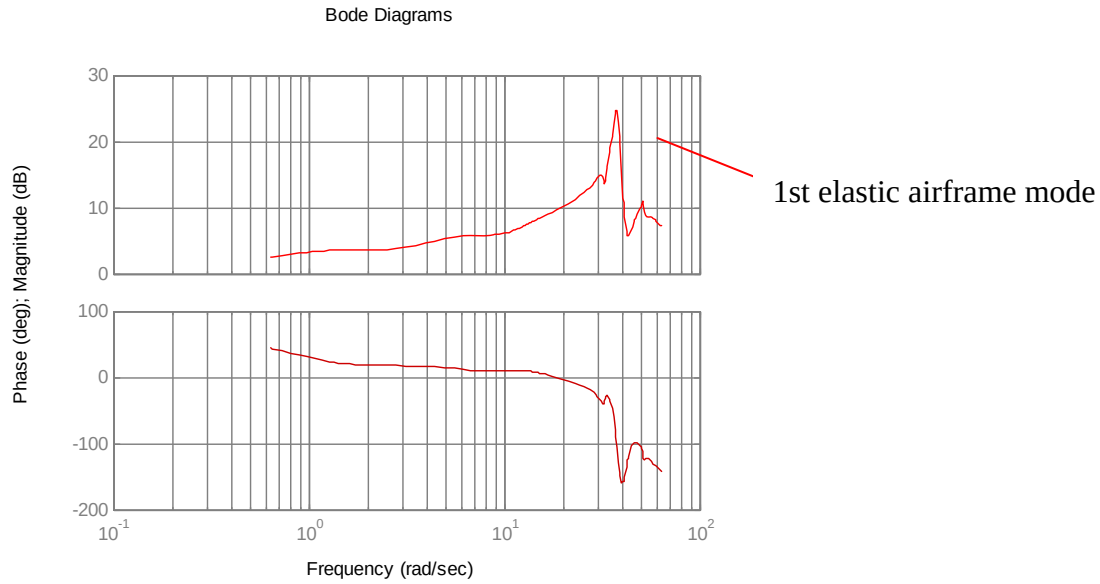

Figure 8: Helicopter transfer function in hover for the pilot seat – ECD

The dynamics of the applied pilot model implemented in transfer function form were extracted from Ref. [11] as at the beginning of the research activities, pilot models were still in development. Please note that 'passive' pilot models are strongly coupled to cockpit and control design issues. Thus the applied pilot model serves as an application example and can neither be generalised nor does it fit to the BO105 cockpit. In figure 9, the root locus plot of the closed loop system is shown for the feedback gain being varied between 0 – i.e. open loop – to one. It can be clearly seen that the poles related to the pilot model are significantly destabilised as expected.

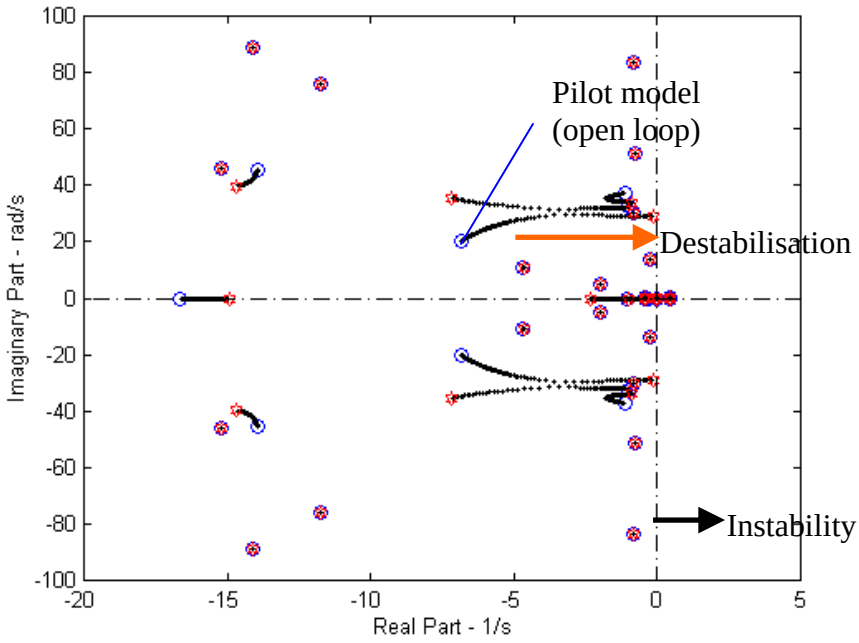

Figure 9: Closed loop system for hover – ECD

Convergence studies have been performed with respect to the complexity of the main rotor and airframe dynamic models. Regarding the BO105 hingeless main rotor system, the consideration of four elastic blade modes proved to be sufficient for the main rotor in order to obtain converged results i.e. damping and frequency of the critical (coupled) mode do not change when adding additional blade modes are added to the plant model. Concerning the

airframe, three elastic airframe modes are adequate for the BO105 numerical test bed using a similar procedure. It is open whether these findings can be easily transferred to other helicopters and other aeroelastic RPC phenomena. In addition the role of unsteady aerodynamics – 2D as well as 3D – on this kind of phenomena was analysed by UROMA3 in depth.

Furthermore parameter variations have been studied with respect to modal airframe frequencies, modal airframe damping, modal airframe mass and operating conditions in order to study sensitivity issues. Finally, the complexity of the vertical bouncing model was increased in a stepwise manner by including actuator dynamics, the cyclic control channels, drive train dynamics and slung loads. For a more detailed review of the research work performed, the reader is referred to Ref. [5].

4.2 'Passive' Pilot Modelling

As mentioned above, the pilot acts as a dynamic component in the feedback loop of the coupled system. A conventional approach to set up a pilot model is to measure the control displacements when the pilot is exposed to known vibrations. Typically this experimental approach is performed under laboratory conditions i.e. the pilot is put on a shaker table where a representative control system – collective lever, cyclic stick and pedals – is installed. Another approach directly using a simulator, as done in this research, is outlined in the next chapter and described in more detail in Ref. [6]. A common way to process the experimental data is to derive transfer functions based on the measurements. Nevertheless, this means that the transfer functions and thus the pilot model are strongly linked to the geometric arrangements and dynamic properties of the controls in the test environment. Therefore, it is usually not possible to extrapolate the pilot models to different cockpits and control layouts. This imposes very strong limitations for this approach.

In order to overcome these limitations, a multibody model of the pilot is under development by Politecnico di Milano. The activities are related to [12] which serves as guideline and database for pilot modelling issues. Its main purpose is to provide a detailed biodynamic model in order to allow the simulation of the pilot's behaviour based on first principles. The model is expected to allow simulations of the behaviour of the pilot without the need to refer to a specific reference condition as necessary when using standard linear transfer functions. This means that the pilot model is intended to be applicable towards a wide range of RPC phenomena are set up and calibrated accordingly. Since the main objective of the first development step is related to pilot-collective interactions, work was focussed on the model of the left arm. For the identification of meaningful biodynamic parameters, inverse dynamics analysis is required to compute forces and moments which the muscles need to generate in order to execute the experimentally measured relative motion of the limbs. A procedure involving a cascade of inverse kinematics and inverse dynamics analysis has been designed. The inverse kinematics needs to be applied for motion estimation at articulation level starting from available measurement. The inverse dynamics analysis needs to be executed afterwards to estimate the actuation forces required to perform the computed joint motions. The impedance of each articulation is finally estimated in terms of the relationship between the estimated motion and torques.

Figure 10 shows a sketch of the multibody pilot model with articulations presented by large spheres and with inertia properties of the rigid body elements presented by small spheres for illustration purposes. It should be noted here that geometric, inertia and impedance properties depend on the size of the pilot which is also affected by sex, age, height and weight of

individuals. In correspondence to the other 'aeroelastic' RPC investigations related to the collective control loop focus was put on the adequate representation of the left arm. A more detailed presentation of the development of the multibody pilot model is given in Ref. [5].

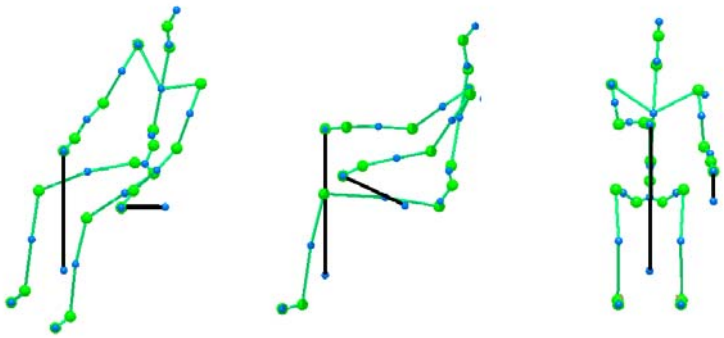

Figure 10: Sketch of the pilot model with hands on controls – POLIMI

5. RPC SIMULATOR TESTING

In order to provide experimental data to the various RPC research activities three different kind of tests were set up and performed using the University of Liverpool's motion base flight test simulator. The tests which will be described below can be sorted as follows:

- 'Rigid body' RPC tests
- Biodynamic tests
- 'Aeroelastic' RPC tests

5.1 'Rigid body' RPC tests

As already mentioned in Section 3, the 'rigid body' RPC tests were used to investigate the applicability of fixed wing RPC criteria and to check the boundaries defined by these criteria. Regarding these tests, the motion base flight simulator was used in a more or less conventional manner with the exception that helicopter models in state space form were imported from outside and not calculated intrinsically as usual. This approach has the following advantages. First, the helicopter model used was identical to that used to generate the 'off-line' predictions. This provides confidence in the validation of the results comparison. Second, helicopter models with several modifications could be easily prepared and imported to the simulator. This was done with respect to the different artificial flight control systems. Another main point in the preparation phase was the set-up of displays and outside-world databases of the simulator for the following piloting tasks:

- Tracking task: bank angle
- Precision hovering: bob-up manoeuvres and side-step manoeuvres
- Slalom manoeuvres
- Pull-up/push-over manoeuvres for the boundary tracking criterion assessment

The pilots were asked to rate each "flown" configuration according to the PIO rating scheme of Hess [13] which is analogue to the well-known Cooper-Harper Rating scale for handling qualities. Afterwards, the ratings were correlated with the predicted results, see for example Table 4 which was set up by the Technical University of Delft analysing the pull-up/push-over manoeuvres in depth. Green marks in the last column identify agreements while red marks indicate dis-agreements in Table 4.

Run	Ft. cond.	Time delay	Pred. PIO	Target freq.	BV	Control strat.	PIOR	✓/x
34	C2	0 ms	No PIO	0.25 Hz	14°	Single axis	1	✓
34	C2	0 ms	No PIO	0.25 Hz	10°	Single axis	1	✓
34	C2	0 ms	No PIO	0.25 Hz	8°	Single axis	1	✓
34	C2	0 ms	No PIO	0.25 Hz	5°	Single axis	1	✓
34	C2	0 ms	No PIO	0.25 Hz	3°	Single axis	1	✓
34	C2	0 ms	No PIO	0.25 Hz	14°	All axes	1	✓
34	C2	0 ms	No PIO	0.25 Hz	5°	All axes	1	✓
16	C2	200 ms	Severe PIO	0.25 Hz	14°	Single axis	2	x
16	C2	200 ms	Severe PIO	0.25 Hz	5°	Single axis	3	x
16	C2	200 ms	Severe PIO	0.25 Hz	3°	Single axis	4	✓
16	C2	200 ms	Severe PIO	0.25 Hz	3°	All axes	5	✓
16	C2	200 ms	Severe PIO	0.5 Hz	5°	Single axis	3-5	✓
16	C2	200 ms	Severe PIO	0.5 Hz	3°	Single axis	5	✓
14	C1	0 ms	No PIO	0.25 Hz	14°	With yaw pedal	1	✓
14	C1	0 ms	No PIO	0.25 Hz	5°	With yaw pedal	1	✓
14	C1	0 ms	No PIO	0.25 Hz	5°	All axes	1	✓
32	C1	200 ms	Moderate PIO	0.25 Hz	14°	All axes	1	x
32	C1	200 ms	Moderate PIO	0.25 Hz	5°	All axes	2/3	✓
32	C1	200 ms	Moderate PIO	0.25 Hz	3°	All axes	2/3	✓
32	C1	200 ms	Moderate PIO	0.375 Hz	5°	All axes	5	x
32	C1	200 ms	Moderate PIO	0.5 Hz	5°	All axes	5	x

Table 4: Predicted PIO susceptibility (Bandwidth Phase Delay criterion) and pilot PIOR – TUD

Performance metrics for the PIO prediction criterion are determined from the simulation tests. The number of cases predicted by the criterion to be PIO prone/free is compared to the actual number of simulator test PIO as shown in the Table 5:

– B is the number of "Pass" cases where both prediction and experimentation agree.

– D is the number of "Fail" cases where both prediction and experimentation agree.

– A is the number of predicted "Pass" cases which "Fail" during the experimentation.

– C is the number of predicted "Fail" cases which "Pass" during the experimentation.

The effectiveness of the PIO criterion in predicting PIO can be evaluated according to the following different effectiveness measures:

– Global success rate = (B+D)/(A+B+C+D) (8)

i.e. the percentage of cases which are correctly predicted to be PIO free or prone.

– Index of conservatism = D/(C+D) (9)

i.e. the percentage of cases predicted PIO prone which have actually undergone PIO in reality with respect to the total number of predicted PIO prone cases.

– Safety index = D/(A+D) (10)

i.e. the percentage of cases which are predicted by the criterion to be PIO prone, with respect to the total number of simulator test PIO cases.

Number of Cases		Simulator test PIO	
		No PIO	PIO
PIO prediction	No PIO	B	A
	PIO	C	D

Table 5: Evaluation of PIO prediction

Assuming PIOR ≤ 2 means No PIO while PIOR > 2 means PIO Table 4 leads to the following values: A = 0, B = 10, C = 2, D = 9 and thus to a global success rate of 90%, an index of conservatism of 82% and a safety index of 100%.

5.2. Biodynamic tests

In the biodynamic test campaign, the capability of the simulator to move the base including the entire cockpit was explicitly exploited by feeding pre-defined accelerations to the motion system and analysing the response of the pilot on controls. The major advantage of this test approach is that the same test set-up including cockpit layout can be used on the one hand for experimentally investigating pilot's impedance and on the other hand for aeroelastic RPC tests with pilot-in-the-loop allowing adequate cross-correlations. Therefore, the simulator had to be prepared in different ways: First, control access to the motion base actuators had to be established in a way that the platform of the simulator could be excited by different signals including "coloured" noise. Second, additional external sensor signals – acceleration signals mounted at the pilot's arm, see also Fig. 11 – had to be acquired and synchronised by the data acquisition system.

The test matrix consisted of the following elements

- translational accelerations in x and z-direction
- amplitudes of 0.1g and 0.2g
- collective lever at 10%, 50% and 90% of full deflection locations
- collective lever with and without friction
- sinusoidal excitation scheme (default) or random excitation scheme

Please note that focus was given on the collective control loop for analysis of the vertical bouncing phenomenon.

Figure 11: Experimental test set-up with acceleration sensors applied to the arm of the pilot

Based on the results obtained, pilot transfer functions were established in a post-processing step – see Fig. 12 – and compared with those known from literature showing adequate similarity. Furthermore, the biodynamic test results will serve as database for the set-up of the multibody pilot model mentioned in Section 4.

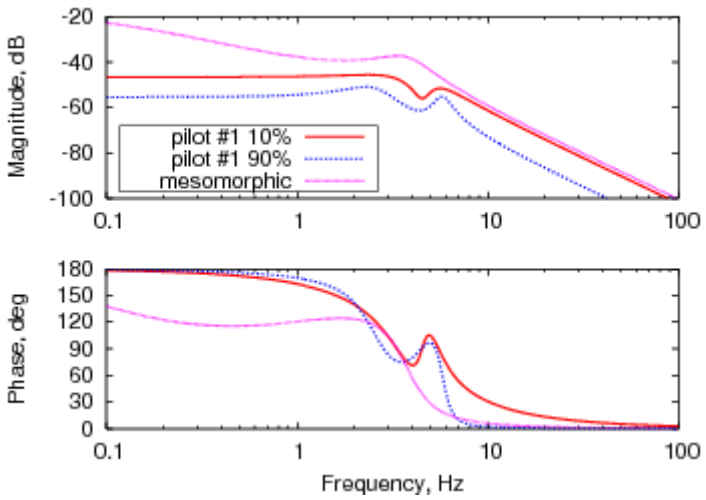

Figure 12: Pilot transfer functions – collective settings 10% and 90% and Mayo's mesomorphic pilot model [11] – POLIMI

5.3 'Aeroelastic' RPC tests

Although not foreseen at the beginning of the research activities, the scope of flight simulator applications was extended to aeroelastic RPC, meaning that the helicopter models implemented in the flight simulator have to be updated in terms of target frequency range. Thus two major issues had to be considered: The implementation of an elastic airframe model and the upgrade of the main rotor system by an elastic hingeless rotor model with adequate number of degrees of freedom. Furthermore, in order to close the aeroelastic loop for the vertical bouncing (and related) phenomena, the accelerations of the motion base need to be modified as well as the accelerations need also to cover the elastic motions of the airframe. Please note that the accelerations fed to the motion base system of the simulator incorporate rigid body accelerations and all elastic accelerations experienced at the pilot seat. The assumption behind this approach is that the simulator itself is very rigid and the motions applied to the pilot seat in the simulator are the same as in the full scale helicopter featuring an elastic airframe. Figure 13 shows the control scheme behind this approach:

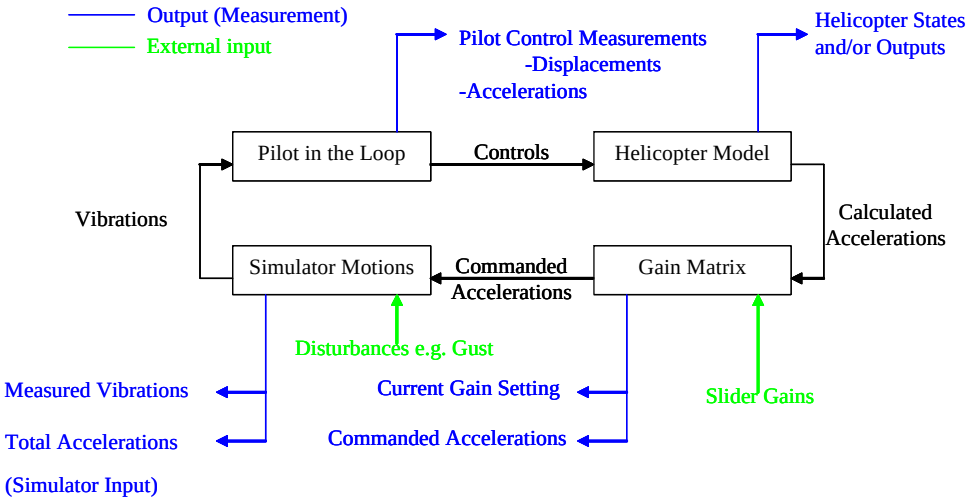

Figure 13: Test scheme for aeroelastic RPC

Focus was given on the implementation of the various components with special care of the elastic airframe and the elastic main rotor. Real time capability might be an issue as the

number of states of the helicopter model increases dramatically with inclusion of airframe and main rotor elastic modes. Furthermore, hardware limitations have to be kept in mind for the high frequency range in order not to overload the simulator. Nevertheless it was demonstrated that such an approach is generally applicable for testing of aeroelastic RPC issues under laboratory conditions.

6. CONCLUSIONS

This paper presents a comprehensive approach analysing different kind of RPC phenomena thus also exploiting synergy effects among the different involved engineering disciplines. The research activities are based on a common test bed, the BO105, which was modified with different kind of degradations in order to provoke related RPC phenomena. Focus was put on low frequency phenomena labelled 'rigid body' RPC and high frequency phenomena labelled 'aeroelastic' RPC highlighting the helicopter dynamic modelling approach. Different methods have been applied to 'rigid body' and 'aeroelastic' RPC with respect to helicopter and pilot modelling as well as the PIO criteria leading to the following conclusions:

'Rigid body' RPC

- A PIO toolbox originally developed for fixed wing aircraft applications in the framework of [8] and [9] was successfully applied to rotorcraft problems.
- The general applicability of fixed wing aircraft PIO criteria to rotorcraft problems was demonstrated for category I and II PIO criteria.
- Accompanying flight simulator test campaigns were used for the assessment of the PIO criteria.
- It is open whether minor adjustments of the boundaries contained within the various PIO criteria are needed. In order to answer this question, the database has to be significantly enlarged by the inclusion of
    - more data points, more pilots and other missions
    - other simulators
    - other aircraft models

'Aeroelastic' RPC

- The vertical bouncing problem was analysed in depth as a representative 'aeroelastic' RPC problem including parameter studies in order to identify main parameters.
- The 'passive' pilot model was identified as key element for 'aeroelastic' RPC. Unfortunately the pilot model is strongly linked to cockpit and controls design and extrapolation using conventional methods is difficult.
- Identification of a pilot model using the simulator as shaker table showed good agreement with models published in literature.
- The development of a multibody pilot model has started aiming on the usage for general cockpit configurations and thus on true predictive capabilities.

Flight simulator testing

- Three different kind of test campaigns have been performed demonstrating the high value of a 6dof motion base simulator for different kind of RPC investigations
    - 'Rigid body' RPC test campaign for verification of fixed wing aircraft PIO criteria
    - Biodynamic tests for identification of 'passive' pilot behaviour by measuring pilot arm and pilot seat accelerations as well as control motions

    - Development of test methodology for simulating ‘aeroelastic’ RPC and performance of functional tests proving the selected approach
- RPC phenomena were investigated under laboratory conditions i.e. with well defined helicopter state space models eliminating uncertainties in the representation of the helicopter.
- The high flexibility in modifying and loading the underlying helicopter models was beneficially used e.g. for variation of helicopter dynamics or inclusion of time delays.

At the time of editing this paper, the research activities are close to finalisation. In the final phase, focus will be put on guidelines and recommendations for RPC prevention.

7. ACKNOWLEDGEMENTS

The provision of the PIO toolbox developed and maintained by GARTEUR FM AG-12 and AG-15 is well appreciated by the group. The work conducted using the University of Liverpool flight simulation facility was supported by a grant from the UK Engineering and Physical Sciences Research Council (Standard Research Grant EP/D003512/1). Special thanks also go to the test pilots who participated in the research.

8. REFERENCES

[1] D.T. McRuer, R.E. Smith *“PIO-A Historical Perspective”*, AGARD –AR-335

[2] D. Hamel *“Rotorcraft-Pilot Coupling: A Critical Issue for Highly Augmented Helicopters”*, AGARD-CP-592, May 1996

[3] R. Barry Walden *“A Retrospective Survey of Pilot-Structural Coupling Instabilities in Naval Rotorcraft”*, 63rd AHS Annual Forum, Virginia Beach, VA, 2007

[4] M.D. Pavel, B.D. Dang Vu, J. Goetz, M. Jump, O. Dieterich, H. Haverdings, *“Adverse rotorcraft-pilot coupling: Prediction and supression of rigid body RPC”*, 34th European Rotorcraft Forum, Liverpool, UK, 2008

[5] M. Gennaretti, J. Serafini, P. Masarati, G. Quaranta, O. Dieterich, *“Aeroelastic and biodynamic modelling for stability analysis of rotorcraft-pilot coupling phenomena”*, 34th European Rotorcraft Forum, Liverpool, UK, 2008

[6] M. Jump, S. Hodge, B. Dang Vu, P. Masarati, G. Quaranta, M. Mattaboni, M. Pavel, O. Dieterich, *“Adverse rotorcraft-pilot coupling: The construction of the test campaigns at the University of Liverpool”*, 34th European Rotorcraft Forum, Liverpool, UK, 2008

[7] J. Stoppel, M. Degener *“Investigations of helicopter structural dynamics and a comparison with ground vibration tests”*, 6th European Rotorcraft Forum, Bristol, UK, 1980

[8] GARTEUR FM AG-12, *“Pilot-in-the-loop oscillations analysis and test techniques for their prevention – phase I”*, Workshop October 11, 2001, EADS, Manching, Germany

[9] GARTEUR FM AG-15, *"Pilot-in-the-loop oscillations analysis and test techniques for their prevention – phase II"*, Workshop May 10, 2007, Saab AB, Linköping, Sweden

[10] National Research Council, *"Aviation safety and pilot control – Understanding and preventing unfavourable pilot-vehicle interactions"*, National Academy Press, Washington D.C., 1997

[11] J.R. Mayo, *"The involuntary participation of a human pilot in a helicopter collective control loop"*, 15th European Rotorcraft Forum, Amsterdam, NL, 1989

[12] H. Cheng, L. Obergefell, A. Rizer, *"Generator of body data (GEBOD) manual"*, Armstrong Laboratory Report No. AL/CF-TR-1994-0051, Wright-Patterson Air Force Base OH, March 1994

[13] R.A: Hess, *"Unified theory for aircraft handling qualities and adverse aircraft-pilot coupling"*, Journal of Guidance, Control and Dynamics, Vol 20, No. 6, November-December 1997